SYNTHESIS AND CHARACTERIZATION OF HIGH ENTROPY ALLOYS FOR HIGH TEMPERATURE APPLICATIONS

M. T. OLARU[1*], D. MITRICA[1], V. SOARE[1], I. CONSTANTIN[1], M. BURADA[1], D. DUMITRESCU[1], A. CARAGEA[1], B. A. CARLAN[1], C. I. BANICA[1], F. STOICIU[1], V. BADILITA[1], V. GEANTA[2], R. STEFANOIU[2]

Present research work investigates the structure and properties of $Al_{0.5}CrFeNiZr_{1.5}Co_{0.5}$, $Al_{0.5}CrFeNiTiSi_{0.4}Nb$ and $Al_{0.7}CrFeNiTiSi_{0.4}Nb$ high entropy alloys. The alloy specimens were prepared by induction melting and were characterized by structural, mechanical and oxidation techniques. The Si and Nb alloys exhibited fine equiaxed dendrites, instead the Zr and Co based alloys exhibited elongated dendrites sprinkled with hard phase particles. X-ray analysis for the $Al_{0.5}CrFeNiTiSi_{0.4}Nb$ alloy has shown a biphasic Laves type structures with slightly different cell parameters. The microhardness analysis showed higher values for Nb alloys (1250HV) and a more uniform distribution of microhardness across the Co based specimen section. Both alloys have superior hardness, comparable to cast iron or high-grade stainless steels. The oxidation resistance tests at 1100ºC showed parabolic behaviour with good oxidation resistance for alloys containing Ti, Si and Nb.

Keywords: materials science, high entropy alloys, characterization, oxidation resistance

1. Introduction

Alloys are traditionally based on a single element with minor additions of other elements to improve specific properties. In this manner the alloys are named after the major element in the alloy. High entropy alloys (HEA) represent a new class of multicomponent alloys composed of minimum 5 elements, in equimolar or near-equimolar ratio. Due to the large mixing entropy of HEA the formation of intermetallic compounds is restrained, and simple solid solution structures prevail. The absence of a matrix element makes each element to be considered as a solute. Normally, the atomic fraction of each component is higher than 5 at.%. The multicomponent equimolar alloys should be located in the middle of the phase

[1] National R&D Institute for Nonferrous and Rare Metals – IMNR, Ilfov, Romania; *corresponding author's e-mail: o.mihai@imnr.com

[2] Faculty of Applied Chemistry and materials Science, University POLITEHNICA of Bucharest, Romania

diagram and their configurational entropy of mixing reaches its maximum when solid solution phase is formed. High entropy alloys have several excellent physical and chemical properties such as high hardness, high mechanical strength, good wear and corrosion resistance at high temperatures. Typically, HEAs have high melting points and a superior yield strength, which can be maintained at very high temperatures. The properties of the alloys used for various applications depend largely on their composition. The structure types are the dominant factor for controlling the strength of the high entropy alloys. By the substitution of one or more elements in HEA composition, significant changes in properties can be obtained. Also, the decrease or increase in the proportion of the alloying elements leads to different structures with important influences on the properties of the alloys. Due to the large number of possible combinations of elements that can be used for HEA synthesis, several thermodynamic criteria were developed for selection of most appropriate HEA compositions for required properties[1-6].

2. Experimental

HEA ingots with defined composition were prepared using induction melting of commercially pure metals (purity greater than 99%) in a high purity argon atmosphere.

Pure metal chunks were cleaned in isopropyl alcohol for 5 minutes in an ultrasonic bath, then dried and melted at high temperature between 1600 ÷ 2100°C, under argon pressure of 0,6÷0,8 bar, in an alumina-magnesium crucible. The ingots were cast in cold copper mould under inert argon atmosphere, resulting in cylindrical rods with 20 mm in diameter and 120 mm in length. The chemical composition of the alloys was determined by optical emission spectrometry in inductively coupled plasma (ICP-OES) using an Agilent 725 spectrometer. Optical microscopy investigation was performed with a Zeiss Axio Scope A1m Imager microscope. Samples were previously etched in 1 to 3 cc HF, 4 cc HNO_3, 100 cc H_2O solution to enhance the visibility of the grains and the grain boundaries.

The crystalline structure was analysed by X-ray diffractometry (XRD). Data acquisition was performed on BrukerD8ADVANCE diffractometer using Bruker DIFFRACPlus software, Bragg–Brentano diffraction method, H–H coupled in vertical configuration, with the following parameters: Cu Ka radiation, 2H region: 2041240, 2H step: 0.020, time/step: 8.7 s/step. Cu Kb radiation was removed with SOL X detector. Resulted data was processed using Bruker DIFFRACPlus EVA v12 software to search the database ICDD powder diffraction file (PDF-2, 2006 edition) and the full pattern matching (FPM) module of the same software package. FPM is a global fitting of the measured scan. FPM

allows the identification of average crystallite size and refinement of lattice parameters.

Microhardness of selected alloys were measured with Anton Paar MHT10 equipment applying 2N of force with 0,6N/s speed attached to a Zeiss AxioImager A1m optic microscope. Three indentations were made for each type of alloy.

Oxidation resistance tests were performed at various temperatures for different periods of time. After the heat treatment the samples were weighted to determine the mass variation before and after oxidation resistance tests.

Table 1 presents the nominal atomic composition of prepared alloys. The induction melted charges were of 300 – 500g.

Table 1

Nominal chemical composition of induction melting prepared alloys

Alloy	Composition, %wt.									
	Al	**Co**	**Cr**	**Zr**	**Fe**	**Mo**	**Ni**	**Ti**	**Nb**	**Si**
$Al_{0.5}CrFeNiTiSi_{0.4}Nb$	3.76	-	14.48	-	15.55	-	16.34	13.33	25.86	10.68
$Al_{0.7}CrFeNiTiSi_{0.4}Nb$	5.18	-	14.26	-	15.31	-	16.1	13.13	25.48	10.53
$Al_{0.5}CrFeNiZr_{1.5}Co_{0.5}$	3.90	8.50	15.01	39.50	16.13	-	16.95	-	-	-

3. Results and discussion

The prepared ingots were analysed by ICP-OES to determine the chemical composition. Samples from different areas of the ingots were analysed. The mean results of the analysis are shown in table 2.

Table 2

Chemical composition of cast ingots

Alloy	Composition, wt . %									
	Al	**Co**	**Cr**	**Fe**	**Mo**	**Nb**	**Ni**	**Ti**	**Si**	**Zr**
$Al_{0.5}CrFeNiTiSi_{0.4}Nb$	3.40	-	14.60	15.85	-	25.39	16.00	13.80	10.40	-
$Al_{0.7}CrFeNiTiSi_{0.4}Nb$	4.90	-	14.48	15.70	-	25.25	15.90	13.50	10.27	-
$Al_{0.5}CrFeNiZr_{1.5}Co_{0.5}$	4.40	8.80	10.80	16.50	-	-	14.60	-	-	44.10

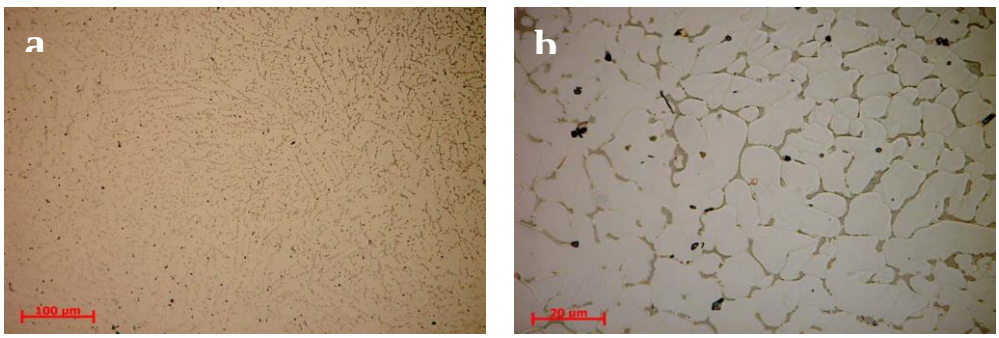

Fig 1. Optical microscopy image of the $Al_{0,5}CrFeNiTiSi_{0,4}Nb$ alloy at different magnification: 200x (a), 900x (b).

Fig. 1 presents the optical microscopy of $Al_{0,5}CrFeNiTiSi_{0,4}Nb$ high entropy alloy showing a fine equiaxed dendritic structure with secondary arms size of less than 20 μm. The inter-dendritic region is significantly reduced.

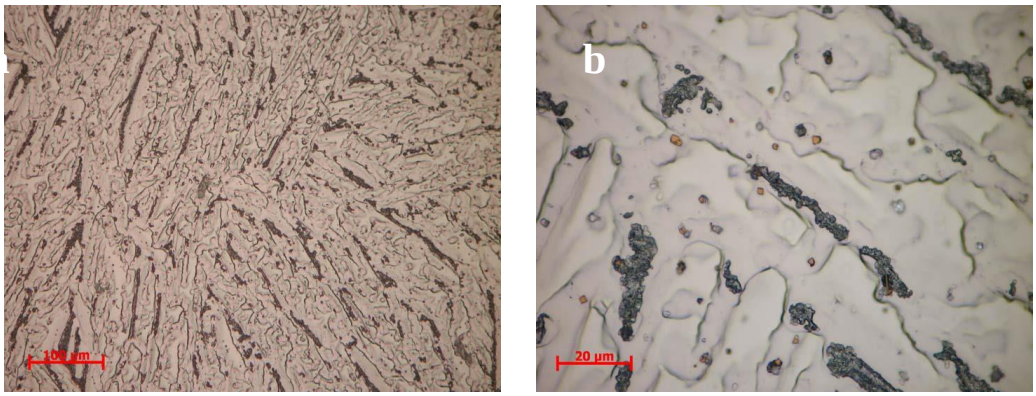

Fig 2. Optical microscopy image of the $Al_{0,5}CrFeNiZr_{1,5}Co_{0,5}$ alloy at different magnification: 200x (a), 900x (b).

Optical microscopy of $Al_{0.5}CrFeNiZr_{1.5}Co_{0.5}$ high entropy alloy (Fig. 2) presents a dendritic microstructure with elongated secondary arms with size of less than 150 μm. A large number of hard particles, which are uniformly spread in the alloy mass, can be found especially in the dendritic area.

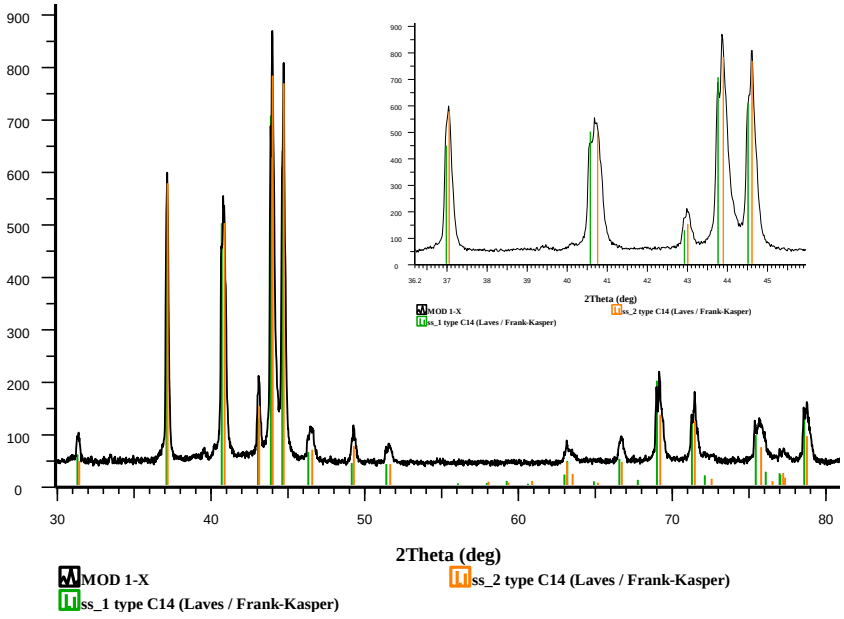

Fig 3. Results of the XRD analysis of $Al_{0,5}CrFeNiTiSi_{0,4}Nb$ high entropy alloy

These types of structures are specific to high entropy alloys obtained by casting in copper mould, due to relatively high cooling speed of the sample.

XRD analysis of $Al_{0,5}CrFeNiTiSi_{0,4}Nb$ (fig. 3 and table 3) cast alloy shows the presence of two Laves phases with very similar lattice constants. These types of complex structures can often be found in titanium-based alloys.

Table 3

Structural characterization of $Al_{0,5}CrFeNiTiSi_{0,4}Nb$ alloy by XRD analysis

Phase	Structure	Lattice constant		D (nm) Scherrer	S-Q (ms.%)
		a (Å)	c (Å)		
Solid Solution C14 type	Hexagonal P63/mmc (194)	4.861	7.847	71	40
Solid Solution C14 type	Hexagonal P63/mmc (194)	4.852	7.805	48	60

The hardness analysis results are presented in table 4. $Al_{0,5}CrFeNiTiSi_{0,4}Nb$ alloy presents higher hardness values, but with significantly differences between measured values across its surface. $Al_{0,5}CrFeNiZr_{1,5}Co_{0,5}$ alloy presents more uniformly distributed hardness values. Both alloys haves high hardness values, comparable with high grade cast iron.

Table 4

Microhardness of selected cast high entropy alloy

Alloy	Microhardness, HV				
	Test 1	Test 2	Test 3	Mean	Standard deviation
$Al_{0,5}CrFeNiTiSi_{0,4}Nb$	1099,9	1273	1400,8	1257,9	123,30
$Al_{0,5}CrFeNiZr_{1,5}Co_{0,5}$	1061,4	1095	1128,6	1095	27,43

The oxidation behaviour of $Al_{0.5}CrFeNiTiSi_{0.4}Nb$, $Al_{0.7}CrFeNiTiSi_{0.4}Nb$ and $Al_{0.5}CrFeNiZr_{1.5}Co_{0.5}$ high entropy alloys were studied. The samples were equally cut, prepared with abrasive paper, cleaned with acetone and heated at 1100°C for 15, 30 and 50 hours in ambient atmosphere. Heating speed was set to 10°C/min. The samples calculated area was 10,5 cm^2. Gravimetric tests were done to evaluate the samples mass loss after the heat treatment. Samples weight was measured with OHAUS Adventure Pro analytical balance. The results are presented in table 5.

Table 5

Weight loss of heat-treated high entropy alloys at 1100°C

Alloy	Δm, mg/cm²		
	15 hours	30 hours	50 hours
$Al_{0.5}CrFeNiTiSi_{0.4}Nb$	4,53	6,07	7,04
$Al_{0.7}CrFeNiTiSi_{0.4}Nb$	6,15	10,62	10,95
$Al_{0.5}CrFeNiZr_{1.5}Co_{0.5}$	114	220,95	333,33

Oxidation resistance of the studied alloys is characterized by the variation of the oxide mass formed on the surface of the material depending on exposure time. Mass-time curves can grow linear meaning a low oxidation protection, also can grow parabolic meaning a good oxidation protection or linear-parabolic descending meaning material loss. From the graphic representation (Fig. 4) a slightly parabolic behaviour can be observed on the alloys with Ti, Si and Nb. $Al_{0.5}CrFeNiZr_{1.5}Co_{0.5}$ has a larger mass gain and linear form of oxidation.

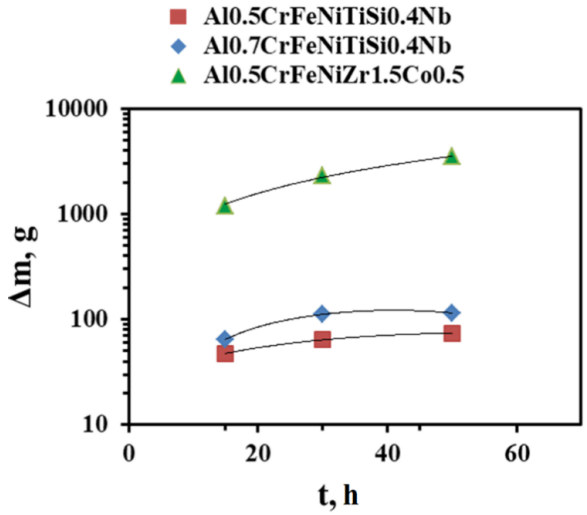

Fig 4. Mass gain vs. time during oxidation tests, carried out in air at 1100°C

It can be concluded that $Al_{0.5}CrFeNiTiSi_{0.4}Nb$ and $Al_{0.7}CrFeNiTiSi_{0.4}Nb$ alloys form a compact and uniform oxide layer, which remains stable during the oxidation process.

4. Conclusions

The microstructural and chemical analysis of presented high entropy alloys show a high homogeneity of the cast samples, with two-phase systems solidified in dendritic structures, of relatively small dimensions. The phases are evenly distributed in the alloy mass. The Al0,5CrFeNiTiSi0,4Nb alloy contains mostly Laves phases. Oxidation resistance experiments for Al0.5CrFeNiTiSi0.4Nb, Al0.7CrFeNiTiSi0.4Nb and Al0.5CrFeNiZr1.5Co0.5 alloys, at 1100 ° C, for 15, 30 and 50 hours have shown good results for the Al0.5CrFeNiTiSi0.4Nb and Al0.7CrFeNiTiSi0.4Nb alloys (increasing parabolic character), and less oxidation resistance for the Al0.5CrFeNiZr1.5Co0.5 alloy (linear increase of oxide mass over time). The results obtained are superior to the alloys currently used in

practice, such as FeCrAl alloy used for components working at temperatures higher than 900-1000°C [11-13].

R E F E R E N C E S

[1] B. S. Murty, J.W. Yeh, S. Ranganathan, High-Entropy Alloys, Butterworth-Heinemann, London, 2014.

[2] J. W. Yeh, Recent Progress in High-entropy Alloys , Annales de Chimie - Science des Matériaux., vol. 31, 2006, pp. 633-648.

[3] Y. Zhang, T. T. Zuo, Z. Tang, M. C. Gao, K. A. Dahmen, P. K. Liaw and Z. P. Lu, Microstructures and properties of high-entropy alloys, Progress in Materials Science, vol. 61, 2014, pp. 1-93.

[4] Michael C. Gao, "Progress in High-Entropy Alloys", Journal of Materials, 2014

[5] Y. Zhang, T. T. Zuo, Z. Thang, M. C. Gao, K. A. Dahmen, P. K. Liaw, Z. P. Lu, "Microstructure and properties of high-entropy alloys", Progress in Materials Science, vol. 61, 2014

[6] M. H. Tsai, J. W. Yeh, "High-Entropy Alloys: A Critical Review", Materials Research Letters, 2014

[6] V. Soare, D. Mitrica, I. Constantin, V. Badilita, F. Stoiciu, A-M. J. Popescu, I. Carcea, Influence of the re-melting on the microstructure, hardness and corrosion behaviour of the AlCoCrFeNiTi high-entropy alloy, Special issue on high entropy alloys, accepted for publication in Materials Science and Technology, Manney, 2015

[7] O.N. Senkov, G.B. Wilks, D.B. Miracle, C.P. Chuang, P.K. Liaw, Refractory high-entropy alloys, Intermetallics, vol. 18, Issue 9, 2010, pp. 1758–1765.

[8] O.N. Senkov, G.B. Wilks, J.M. Scott, D.B. Miracle, Mechanical properties of $Nb_{25}Mo_{25}Ta_{25}W_{25}$ and $V_{20}Nb_{20}Mo_{20}Ta_{20}W_{20}$ refractory high entropy alloys, Intermetallics, vol. 19, issue 5, 2011, Pages 698–706.

[9] O.N. Senkov, C.F. Woodward, Microstructure and properties of a refractory $NbCrMo_{0.5}Ta_{0.5}TiZr$ alloy, Materials Science and Engineering: A, vol. 529, 2011, pp. 311–320.

[10] Z. Tang, M. C. Gao, H. Diao, T. Yang, J. Liu, T. Zuo, Y. Zhang, Z. Lu, Y. Cheng, Y. Zhang, K. A. Dahmen, P. K. Liaw, T. Ehami, "Aluminium Alloying Effects on Lattice Types, Microstructures and Mechanical Behavior of High-Entropy Alloys Systems", Journal of Materials, vol. 65, no. 12, 2013

[11] C.M. Liu, H.M. Wang, S.Q. Zhang, H.B. Tang, A.L. Zhang, "Microstructure and oxidation behaviour of new refractory high entropy alloys", Journal of Alloys and Compounds, vol. 583, 2014

[12] D. Pilone, "Ferritic Stainless Steels for High Temperature Applications in Oxidizing Environments", Recent Patenrs on Materials Science 2009, vol 2, pages 27-31.

[13] R. B. Rebak, V. K. Gupta, M. Larsen, “Oxidation Characteristics of Two FeCrAl Alloys in Air and Steam from 800C to 1300C”, Journal of Materials, vol 70 august 2018